Research Journal of Applied Sciences, Engineering and Technology 7(15): 3145-3149, 2014
DOI:10.19026/rjaset.7.653
ISSN: 2040-7459; e-ISSN: 2040-7467

Submitted: October 20, 2013 Accepted: October 31, 2013 Published: April 19, 2014

Research Article

Comparative Finite Element Analysis of the Effects of Tillage Tool Geometry on Soil Disturbance and Reaction Forces

[1, 2]Mohamed Ahmed Elbashir, [1]Zheng Zhao, [1]Eidam Ahmed Hebeil and [1]Xiaoyu Li
[1]Department of Agricultural Equipments Automation and Measurement Technology, College of Engineering, Huazhong Agricultural University, Wuhan City, Hubei Province, 430070, P.R. China
[2]Department of Agriculture Engineering, Faculty of Agriculture Sciences, University of Gezira, Wad Medani, P.O. Box 20, Republic of the Sudan

Abstract: In this study a comparative finite element analysis was conducted to investigate the effects of tillage tool geometry on soil disturbance and reaction forces. A nonlinear three dimensional finite element model, using ANSYS software, was developed to study the soil cutting process by trapezoidal (T_1) and rectangular (T_2) flat tools that inclined to the horizontal at three rake angles ($R_1 = 30°$, $R_2 = 60°$ and $R_3 = 90°$), therefore a total of six treatments were considered in this analysis. The soil media was assumed as elastic-perfectly plastic material with Drucker-Prager's model. Results of this study revealed that the maximum vertical soil displaced by T_1 is greater than that of T_2; hence T_1 disturbed the soil better than T_2. Results also showed that a significant reduction in draft force was noticed when cutting the soil with T_1 in comparison to T_2. Designing the tool in the form of T_1 significantly reduces the surface area of the tool; thus conserving the engineering material.

Keywords: Draft force, soil cutting simulation, soil disturbance, tillage tool geometry

INTRODUCTION

Tillage is the practice of modifying the state of the soil to achieve favorable conditions to crop growth. It is the most costly farm operation, because of the large amount of energy requirement during soil manipulation. A remarkable saving of that high amount of energy can be attained through optimized design and development of tillage tools (Gill and Vandenberg, 1968). These tools have for a long time been designed on trial and error basis as the soil-tool interactions involved have not been delineated and quantified (Makanga *et al*., 1996).

Tool draft is a force required to overcoming the shearing resistance of the soil. Precise awareness of that force and energy consumption of tillage tools is paramount for proper design of tools, appropriate matching of the tools with their power sources and the selection of the optimum working conditions (Manuwa, 2009). The best way to estimate the energy consumption of a given tool is by estimating its draft requirement under optimum working soil conditions (Ehrhardt *et al*., 2001). The draft force of any tillage tool mainly depends upon the soil properties, tool geometry, working depth, travel speed and width of the tool (Glancey *et al*., 1996).

Several researchers have used both analytical and numerical methods to investigate the soil cutting process and soil-tool interaction. Among the numerical methods, the Finite Element Method (FEM) is proved to be helpful in understanding and describing the subject. In their finite element analysis of soil-tool interaction (Chi and Kushwaha, 1991; Gee-Clough *et al*., 1994; Abo-Elnor *et al*., 2004; Jafari, 2008; Davoudi *et al*., 2008) used rectangular flat tools of different widths. In the previous research, the use of trapezoidal flat tool in the simulation of soil-tool interaction was not presented.

The objective of this study is to develop a finite element model using ANSYS software to simulate the soil cutting process by trapezoidal and rectangular flat tillage tools. Also the other aim of the present study is to investigate the effects of tool geometry on the soil disturbance and reaction forces.

MATERIALS AND METHODS

Finite element formulation: In this research, soil is considered as non-linear elastic-Perfectly plastic material. The elastic-plastic model describes an elastic-perfectly plastic behavior which can be illustrated by a two-stage of stress-strain relationship as shown in Fig. 1. Stage 1, shows the pure elastic behavior where

Corresponding Author: Xiaoyu Li, Department of Agricultural Equipments Automation and Measurement Technology, College of Engineering, Huazhong Agricultural University, Wuhan City, Hubei Province, 430070, P.R. China, Tel.: +86-027-8728-1002; Fax: +86-027-8767-1041

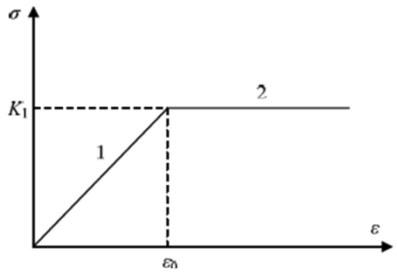

Fig. 1: Elastic-perfectly plastic behavior of soil under uniaxial load

the stresses are directly proportional to the strain until the yield point ε_0, while stage 2 explains the perfectly plastic behavior at which the stress-strain curve is perfectly horizontal. This stress-strain relationship can be expressed by Eq. (1):

$$\sigma = \begin{cases} k_0\varepsilon, 0 \le \varepsilon \le \varepsilon_0 \\ k_1, \varepsilon_0 \le \varepsilon \end{cases} \quad (1)$$

where,
σ = The axial stress
k_0 = Constant
ε = The axial strain
ε_0 = The strain value at joint point where plasticity begins
k_1 = The stress in the perfectly plastic stage

A yield function introduced by Drucker and Prager for the elastic-perfectly plastic material model can be expressed as in Eq. (2) (Mouazen and Nemenyi, 1999a):

$$f = 3\alpha\sigma_m + \bar{\sigma} - k = 0 \quad (2)$$

where, α, k are material parameters and σ_m is the mean compressive stress, that can be written in terms of first stress invariant, I_1, Eq. (3):

$$\sigma_m = \frac{1}{3}I_1 = \frac{1}{3}\left(\sigma_x + \sigma_y + \sigma_z\right) \quad (3)$$

and $\bar{\sigma}$ is the effective stress and can be related to the second stress invariant, J_2, as in Eq. (4):

$$\bar{\sigma} = \sqrt{J_2}$$

in which,

$$J_2 = \frac{1}{2}\left[\left(\sigma_x - \sigma_m\right)^2 + \left(\sigma_y - \sigma_m\right)^2 + \left(\sigma_z - \sigma_m\right)^2\right] + \tau_{xy}^2 + \tau_{yz}^2 + \tau_{xz}^2 \quad (4)$$

where,
τ = The shear stress
σ = The compressive stress

According to Eq. (3) and (4), the Drucker-Prager material model accounts for both volumetric and shear behaviors of soil.

The theory of incremental plasticity is used to formulate soil plasticity. Once a material commences to yield, the incremental total strain can be divided into elastic and plastic strains as:

$$d\varepsilon = d\varepsilon^e + d\varepsilon^p \quad (5)$$

Only elastic strain increments $d\varepsilon^e$ will generate stress changes; hence stress increments can be stated as follows:

$$d\sigma = C_e d\varepsilon^e = C_e\left(d\varepsilon - d\varepsilon^p\right) \quad (6)$$

The yield function (f) is a function of normal and shear stress, therefore an incremental change in that function is given by:

$$df = \frac{\partial f}{\partial \sigma_x}d\sigma_x + \frac{\partial f}{\partial \sigma_y}d\sigma_y + \frac{\partial f}{\partial \sigma_z}d\sigma_z + \frac{\partial f}{\partial \tau_{xy}}d\tau_{xy} = \frac{\partial f}{\partial \sigma}d\sigma \quad (7)$$

According to the theory of incremental plasticity df will be equal to zero when the stress state is on the yield surface. This condition is known as the natural loading condition which can be stated as follows:

$$df = \frac{\partial f}{\partial \sigma}d\sigma = 0 \quad (8)$$

The incremental plastic strain is defined as a function of potential plastic function:

$$d\varepsilon^p = \lambda\frac{\partial g}{\partial \sigma} \quad (9)$$

where,
g = The potential plastic function
λ = The plastic multiplier

Finally at a given incremental strain the incremental stress can be obtained as follows:

$$d\sigma = \left(C_e - C_p\right)d\varepsilon \quad (10)$$

Material and tool properties: A silty loam soil (57% silt, 36% sand and 7% clay) was used as a material in the FEM simulation. The triaxial compression test apparatus (Ke′zdi, 1980) was used to determine soil cohesion, soil internal friction angle, modulus of elasticity and Poisson's ratio. A modified direct shear box (Chi and Kushwaha, 1991) was used to measure soil adhesion and soil-metal external friction angle. For the tool the mechanical properties of steel # 45 was used. The mechanical properties of the soil and soil-tool interface that were used as input data for the FEM model were summarized in Table 1.

Table 1: Mechanical parameters of soil and soil-tool interface used in FEM simulation

Property	Value
Soil mechanical parameters	
Bulk density, ρ	1410 kg/m^3
Soil moisture content, w	12.8% d.b.
Cohesion, c	8.1 kPa
Internal friction angle, ϕ	23.7°
Modulus of elasticity, E	4460 kPa
Poisson's ratio, v	0.342
Soil-metal mechanical parameters	
Soil-metal adhesion, C_a	1.1 kPa
Soil-metal external friction angle, δ	5.7°
Soil-metal coefficient of friction, μ	0.1

Finite element mesh and boundary conditions: The soil media is modeled as a cube of solid material having dimensions of 1000×600×450 mm, (length×width ×height). In the finite element analysis of soil-tool interaction two types of flat tools were used that were trapezoidal flat tool (T_1) and rectangular flat tool (T_2). The top width of the T_1 is the same as that of T_2 (100 mm), while its bottom width is equal to 50 mm. The lengths of the two tools varied according to their respective rake angles (forward angles between tool face and horizontal soil surface) which were set at $R_1 = 30°$, $R_2 = 60°$ and $R_3 = 90°$. The combination of T and R comprises a theoretical experiment of six treatments. Models of soils and T_1 and T_2 were built in UG v 6.0 drawing software and then transferred to ANSYS v 12.1. For the soil, the Drucker-Prager material model with soil mechanical properties shown in Table 1 as inputs was used; while for the tool, the linear elastic isotropic material model with mechanical properties of steel # 45 was used. Solid with 10 nodes, 92 elements was used for meshing both soil and tool. The model was meshed by using the free smart sizing meshing feature in such a way that increased the mesh density at the tool and soil in vicinity of the tool. The soil displacement and failure studied was symmetric about the center line of the tool. Thus only one half of the model was considered in the analysis, but all the results considered the complete model.

To simulate the contact surfaces between the soil and each of the T_1 and T_2, Coulomb's friction model was used. The interface between the soil and tool was modeled by selecting flexible surface-to-surface contacting (contact and target element) (Fig. 2).

The boundary conditions applied to the soil-tool models were as follows:

- Five faces of the soil media were constrained so that they couldn't move normal to their faces.
- The upper face of the soil was free of constrain.
- The tool is constrained in the vertical direction and from any rotation but it is free to move horizontally along Z axis.

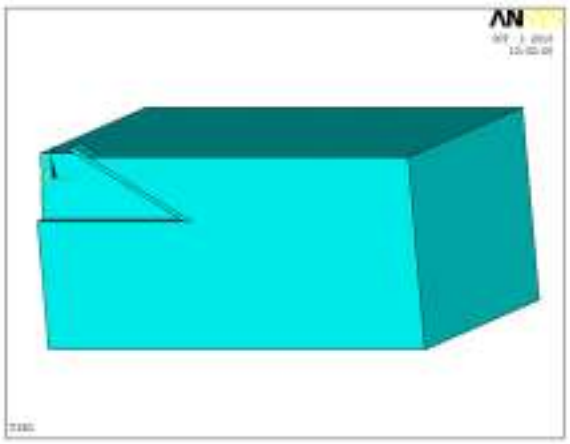

Fig. 2: Soil-T_1R_1 tool interface model

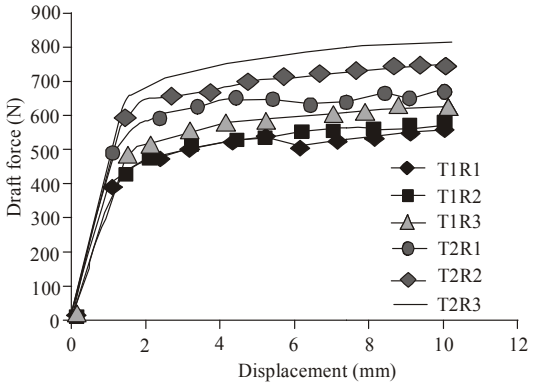

Fig. 3: FEM calculated draft forces against displacement for the six treatments investigated

RESULTS AND DISCUSSION

Results of the finite element analysis at a soil cutting depth of 150 mm provided following information regarding soil reaction forces (draft and vertical forces) and soil displacement fields. The soil reaction forces on the tools were calculated from the summation of the nodal forces on the soil-tool interface elements in the horizontal direction.

Soil reaction forces: Among the soil reaction forces, draft is the most important force which directly related to the energy consumption of tillage operation. Figure 3 illustrates the FEM calculated draft forces against displacement for the six treatments investigated. This draft force increased with the increase in displacement until it reached a maximum value. This maximum draft is considered as the force needed for the failure of the soil block in front of the tool. The vertical forces were taken at this failure level (Fig. 4). From Fig. 3, it is clear that increasing the tool rake angle increased the draft forces for all the treatments studied. The outcomes of this study showed that changing the geometry of the tool resulted in a significant reduction in the draft

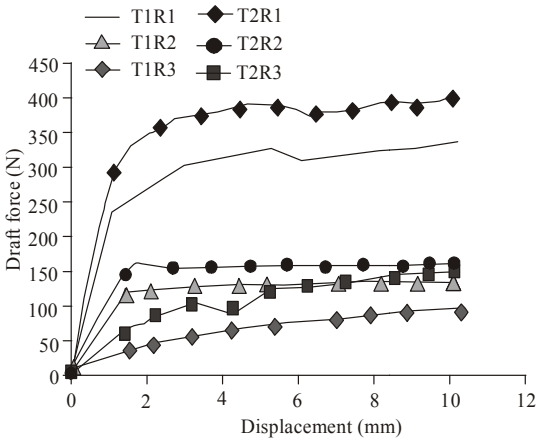

Fig. 4: FEM calculated vertical forces against displacement for the six treatments investigated

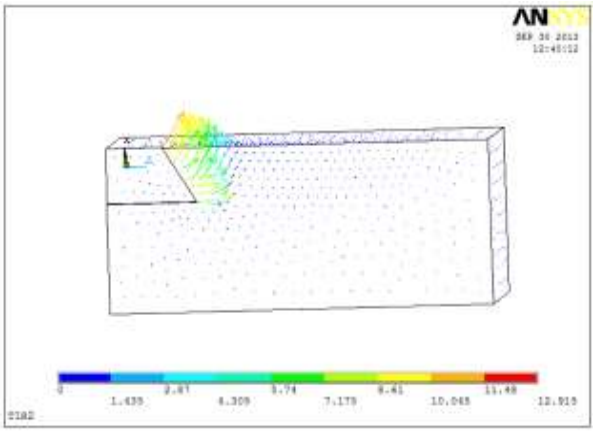

Fig. 5: Soil node displacement vectors when tilled by T_1R_2 tool (displacements are in mm)

forces. At the three rake angles (R_1, R_2 and R_3) the calculated draft force of T_1 was less than that of T_2 by amount of 18.5, 29.7 and 29.8%, respectively. Since energy consumption of tillage tools is draft force dependence, cutting the soil with T_1 would require the least amount of energy. It was also found that at the three rake angles the surface area of T_1 is less than that of T_2 by values of 40.0, 44.4 and 52.4%, respectively. Thus designing of a tool in T_1 form would require less material and conserving the engineering resources.

Soil displacement field: The type and degree of soil disturbance is the main factor in the selection of tillage tools, but this must be considered together with the required draft force for efficient tillage (Godwin, 2007). The distribution of the vertical and forward soil displacement fields were calculated from the FEM model after 10 mm of tool displacement. In the zone cited above the tool, large movements occurred in both horizontal (z) and vertical (x) directions and there was very little lateral (y) displacement. Such arbitrary motions indicated that shear distortion occurred throughout the zone (Mouazen and Nemenyi, 1999b). Figure 5 shows the soil node displacement vectors when the soil was cut by T_1R_2 as an example. The movements of the soil in the z, x and y directions indicated that T_1 and T_2 could cut, loose and turn the soil.

Table 2: Maximum value of soil node displacement vectors (mm) in front of tillage tools investigated

	Tillage tool	
Rake angle	T_1	T_2
30°	8.985	8.748
60°	12.915	12.065
90°	15.428	13.766
Mean soil node displacement vector	12.443	11.526

Comparing the maximum values of soil node displacement vectors, at the three rake angles, showed that T_1 could move the soil vertically more than T_2 (Table 2); hence cutting the soil with T_1 resulted in better soil disturbance than with T_2.

CONCLUSION

A comparative theoretical finite element analysis, using ANSYS software, was conducted to investigate the effects of tillage tool geometry on soil disturbance and reaction forces. The soil was considered as completely homogenous and modeled on the basis of the Drucker-Prager's elastic-perfectly plastic model. The soil cutting process was simulated using a trapezoidal (T_1) and rectangular (T_2) flat tools that inclined to the horizontal at three rake angles (R_1 = 30°, R_2 = 60° and R_3 = 90°). Based on the results of this study, some concluding remarks could be made as follows:

- Cutting the soil with the trapezoidal flat tool significantly reduces the draft force in comparison to the rectangular one.
- Maximum vertical soil displaced by trapezoidal flat tool is greater than that displaced by the rectangular flat tool.
- Trapezoidal flat tool consumed less energy in comparison to the rectangular one and at the same time resulted in a better soil disturbance.
- Designing the tillage tools in a trapezoidal form required less material compared to rectangular one.

REFERENCES

Abo-Elnor, M., R. Hamilton and J.T. Boyle, 2004. Simulation of soil-blade interaction for sandy soil using advanced 3D finite element analysis. Soil Till. Res., 75: 61-73.

Chi, L. and R.L. Kushwaha, 1991. Three-dimensional finite element interaction between soil and simple tillage tool. T. ASAE, 34(2): 361-366.

Davoudi, S., R. Alimardani, A. Keyhani and R. Atarnejad, 2008. A two dimensional finite element analysis of a plane tillage tool in soil using nonlinear elasto-plastic model. Am. Eurasian J. Agric. Environ. Sci., 3(3): 498-505.

Ehrhardt, J.P., R.D. Grisso, M.F. Kocher, P.J. Jasa and J.L. Schinstock, 2001. Using the veris electrical conductivity cart as a draft predictor. ASAE, St. Joseph, Mich.

Gee-Clough, D., J. Wang and W.K. Nukulchai, 1994. Deformation and failure in wet clay soil: Part 3, Finite element analysis of cutting of wet clay by tines. J. Agric. Eng. Res., 58: 121-131.

Gill, W.R. and G.E. Vandenberg, 1968. Soil Dynamics in Tillage and Traction. Agricultural Handbook No. 316, Washington, Dc.

Glancey, J.L., S.K. Upadhyaya, W.J. Chancellor and J.W. Rumsey, 1996. Prediction of agricultural implement draught using an instrumented analog tillage tool. Soil Till. Res., 37: 47-65.

Godwin, R.J., 2007. A review of the effect of implement geometry on soil failure and implement forces. Soil Till. Res., 97: 331-340.

Jafari, R., 2008. Sensitivity analysis of factors affecting on finite element analysis in soil-tool interaction. Proceedings of the 1st WSEAS International Conference on Finite Differences-finite Elements-finite Volumes-boundary Elements (F-and B'08), pp: 22-127.

Ke′zdi, A′., 1980. Handbook of Soil Mechanics: Soil Testing. Elsevier, Amsterdam.

Makanga, J.T., V.M. Salokhe and D. Gee-Clough, 1996. Effect of tine rake angle and aspect ratio on soil failure patterns in dry loam soil. J. Terramechanics, 33(5): 233-252.

Manuwa, S.I., 2009. Performance evaluation of tillage tines operating under different depths in a sandy clay loam soil. Soil Till. Res., 103: 399-405.

Mouazen, A.M. and M. Nemenyi, 1999a. Finite element analysis of subsoiler cutting in non-homogeneous sandy loam soil. Soil Till. Res., 51: 1-15.

Mouazen, A.M. and M. Nemenyi, 1999b. Tillage tool design by the finite element method: Part 1. Finite element modeling of soil plastic behavior. J. Agric. Eng. Res., 72: 37-51.